Proc. Natl. Acad. Sci. USA
Vol. 88, pp. 8764–8768, October 1991
Biochemistry

X-ray structure of trypanothione reductase from *Crithidia fasciculata* at 2.4-Å resolution

(glutathione reductase/oxidative stress/trypanosomiasis/protein crystallography/drug design)

JOHN KURIYAN*†, XIANG-PENG KONG†, T. S. R. KRISHNA*†, ROBERT M. SWEET‡, NICHOLAS J. MURGOLO§, HELEN FIELD§, ANTHONY CERAMI§, AND GRAEME B. HENDERSON§¶

*Howard Hughes Medical Institute and †Laboratory of Molecular Biophysics, and §Laboratory of Medical Biochemistry, The Rockefeller University, 1230 York Avenue, New York, NY 10021; and ‡Department of Biology, Brookhaven National Laboratory, Upton, NY 11973

Communicated by Martin Karplus, July 5, 1991

ABSTRACT **Trypanosomes and related protozoan parasites lack glutathione reductase and possess instead a closely related enzyme that serves as the reductant of a bis(glutathione)-spermidine conjugate, trypanothione. The human and parasite enzymes have mutually exclusive substrate specificities, providing a route for the design of therapeutic agents by specific inhibition of the parasite enzyme. We report here the three-dimensional structure of trypanothione reductase from *Crithidia fasciculata* and show that it closely resembles the structure of human glutathione reductase. In particular, the core structure surrounding the catalytic machinery is almost identical in the two enzymes. However, significant differences are found at the substrate binding sites. A cluster of basic residues in glutathione reductase is replaced by neutral, hydrophobic, or acidic residues in trypanothione reductase, consistent with the nature of the spermidine linkage and the change in overall charge of the substrate from −2 to +1, respectively. The binding site is more open in trypanothione reductase due to rotations of about 4° in the domains that form the site, with relative shifts of as much as 2–3 Å in residue positions. These results provide a detailed view of the residues that can interact with potential inhibitors and complement previous modeling and mutagenesis studies on the two enzymes.**

A promising route toward finding improved therapeutic agents for diseases caused by trypanosomes and leishmanias is to identify differences between the metabolism of the parasite and the host and to develop inhibitors of enzymes specific to the parasite (1, 2). Trypanosomes and leishmanias do not possess the flavoenzyme glutathione reductase (GR), which is found in most aerobic organisms and catalyzes the reduction by NADPH of oxidized glutathione (GSSG) to two molecules of γ-glutamylcysteinylglycine (γ-Glu-Cys-Gly) (2, 3). These parasites rely instead on a bis(glutathione)-spermidine conjugate, trypanothione [$T(S)_2$] (Fig. 1) (2). Oxidized $T(S)_2$ is reduced by the action of trypanothione reductase (TR), a flavoprotein disulfide reductase that is closely related to GR (5). TR was first characterized from an insect trypanosomatid, *Crithidia fasciculata*, and is very similar to GR in size, catalytic mechanism, and amino acid sequence (5, 6). Both enzymes are dimeric and act by transferring electrons from NADPH to an enzyme disulfide by way of FAD, followed by disulfide interchange with the substrate (5). However, human GR and TR are mutually exclusive with regard to substrate (7). This, combined with the known susceptibility of trypanosomatids to oxidative stress when GSSG synthesis is blocked (8, 9), makes TR a promising target for the development of inhibitors that do not react with the host enzyme.

Insight into the basis of substrate discrimination in these enzymes has been obtained by studies on the reduction by TR of $T(S)_2$ analogs (7) and by site-directed mutagenesis and molecular modeling of TR and GR (10–13). These studies have been aided greatly by the x-ray structures of GR (at 1.54-Å resolution) and GR complexed with NADPH and GSSG (at 2-Å resolution) that have been determined by Schulz and coworkers (4, 14, 15). However, a complete understanding of the molecular basis for the altered specificities of the human and parasite enzymes requires direct structural information for the latter. We present here the x-ray structure of TR from *C. fasciculata* (16) at 2.4-Å resolution in the absence of $T(S)_2$.‖

METHODS

TR was purified as described (5) but with the incorporation of an additional ion-exchange chromatography step (Mono-Q, Pharmacia) that resulted in the separation of three closely spaced peaks containing TR activity. All three peaks yield similar well-ordered crystals (16). Characterization of these crystals revealed a slightly different crystal form which was used for the structure determination (form III, $P2_1$, a = 60.0 Å, b = 161.8 Å, c = 61.5 Å, β = 104.1°, dimer in the asymmetric unit). Data collection was carried out at station X12-C of the National Synchrotron Light Source at Brookhaven, using a FAST area detector (Enraf-Nonius, Delft, The Netherlands), with x-rays of 1.1-Å wavelength. Intensities were accumulated over 0.1° rotations, using exposure times ranging from 10 to 20 sec. Strong diffraction was observed to 2-Å resolution. We merged 131,449 measurements of 42,201 unique reflections to 2-Å resolution with an overall error [$R_{sym}(I)$] of 0.079% (17, 18). The final data set is 88% complete to 3 Å, 76% complete between 3 Å and 2.4 Å, and only 35% complete between 2.4 and 2.0 Å. Finally, only data from 10 Å to 2.4 Å were used in the structure solution by molecular replacement, and data from 6 Å to 2.4 Å were used for the refinement of the structure.

Structure determination by molecular replacement used the 1.5-Å structure of GR (13) as a search model with no changes in the sequence and with all protein and FAD atoms included. Calculations were carried out using the programs X-PLOR (19) and MERLOT (20). A three-dimensional rotation function was calculated using a dimer of GR and x-ray data for TR to 4.5-Å resolution (19). The highest two peaks in the

The publication costs of this article were defrayed in part by page charge payment. This article must therefore be hereby marked "*advertisement*" in accordance with 18 U.S.C. §1734 solely to indicate this fact.

Abbreviations: GR, glutathione reductase; TR, trypanothione reductase; GSSG, glutathione; $T(S)_2$, trypanothine.

¶Deceased, September 24, 1990.

‖The atomic coordinates and structure factors have been deposited in the Protein Data Bank, Chemistry Department, Brookhaven National Laboratory, Upton, NY 11973 (reference 2TPR, R2TPRSF).

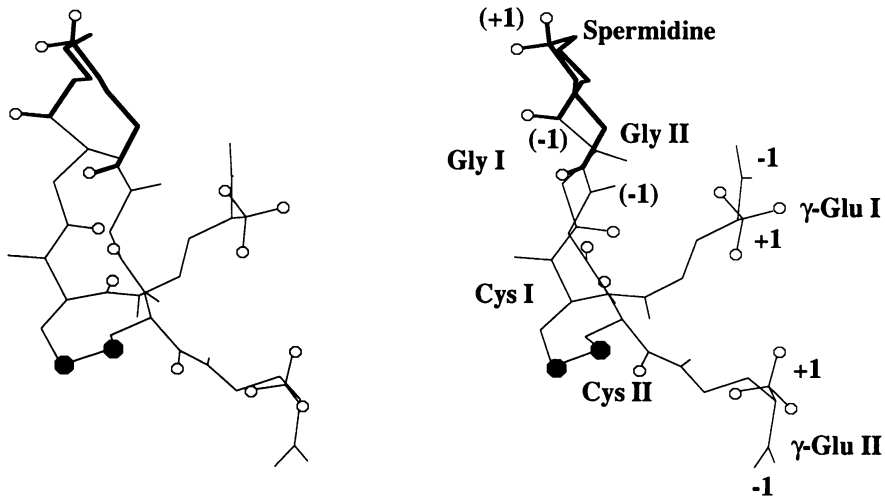

FIG. 1. Stereodiagram of $T(S)_2$. The molecule is shown in the same orientation as in Figs. 3 and 4. The two tripeptides of GSSG are labeled I and II (4). The spermidine crosslink between the glycine residues is shown in thicker lines. Hydrogens bonded to nitrogens are shown as open circles. Formal charges are indicated by the positive and negative numbers, with the charges that differ between GSSG and $T(S)_2$ in parentheses [+1 in $T(S)_2$ and −1 in GSSG].

rotation function were at 4 standard deviations (σ) above the mean and were related by a twofold rotation axis. The orientation was further refined by Patterson-correlation refinement (19), treating the entire dimer as a rigid body and with final correlation coefficients of 0.08 and 0.09 for these two peaks and 0.06 for the next highest. A two-dimensional translation function (19) revealed a single sharp peak with a height of 8σ above the mean. With reference to the GR model, the orientation of the TR molecule in form III crystals corresponds to eulerian rotations of $\theta_1 = 164°$, $\theta_2 = 68°$, $\theta_3 = 100°$, with translations along **a** and **c** of 0.306 and 0.016 in fractional coordinates, respectively.

A combination of model building using FRODO (21) and conventional least-squares refinement using X-PLOR (22) allowed most of the changes in the TR sequence (5) to be built, and the conventional crystallographic residual error (R) value dropped from 52.5% to 28.9% at 2.4-Å resolution. At this stage, x-ray-restrained molecular dynamics refinement (23) was carried out using a previously described protocol (24). A strong indication of the correctness of the model was the presence of readily interpretable electron density for insertions in the TR sequence (Fig. 2). The current model includes 3681 nonhydrogen protein and FAD atoms per subunit and 128 water molecules. The R value is 19.1% for 33,134 reflections between 6 Å and 2.4 Å, with $|F| > 2\sigma(|F|)$, where F is the structure factor. The rms deviation of bond lengths and angles from ideality is 0.019 Å and 3.5°, respectively. There are two residues with no backbone density to accommodate them (residues 131–132) in an insertion in the TR sequence on the surface of the molecule. The next 15 residues (residues 133–147) have poor side-chain density and have been built as alanine residues. In addition, the last 6 residues of the C terminus are not well-ordered and have not been included.

RESULTS AND DISCUSSION

The *C. fasciculata* TR sequence is very similar to that of *Trypanosoma congolense* TR, with an overall sequence identity of 68% (6, 25). The similarity to human GR is much lower, with 34% identity. Both TR sequences lack the 17 N-terminal residues that are disordered in the GR x-ray structure and possess a C-terminal extension (19 residues in *C. fasciculata*). There are two insertions relative to GR that are longer than three residues in both TR sequences: TR residues 38–46, between GR residues 53 and 54, and TR residues 129–139, between residues 133 and 134 in GR (6).

The structure of TR closely resembles that of GR, as expected. The enzyme is dimeric, with two symmetrical active sites. Each monomer consists of four domains: the N-terminal FAD binding domain, the NADPH binding domain, the central domain that also provides part of the FAD binding site, and the C-terminal interface domain. Each substrate binding site is a deep crevice, at the base of which is located the redox-active disulfide of the enzyme and below the disulfide is the flavin ring system. One side of the crevice includes three helices from the FAD and central domains and on the other side are strands of β-sheet and an α-helix from the interface domain of the other monomer (Fig. 3).

The structure of TR has been determined in the absence of $T(S)_2$, and all comparisons in the following discussion are with the 1.5-Å resolution structure of GR in the absence of

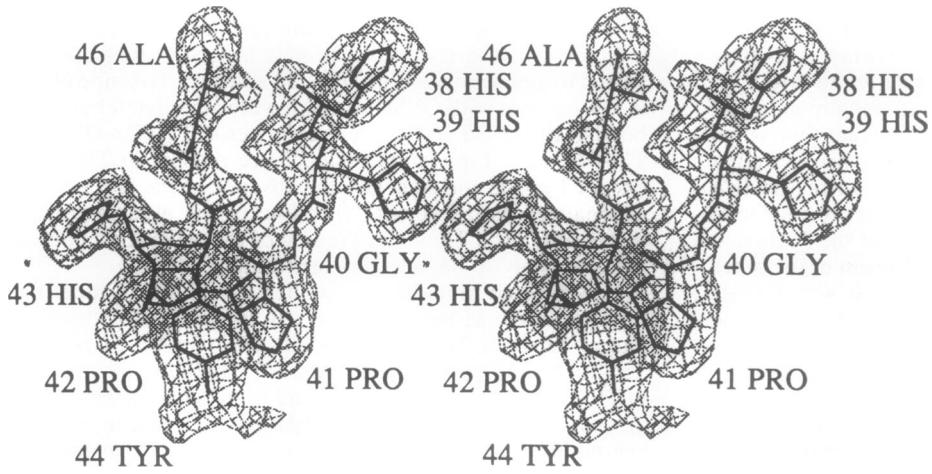

FIG. 2. Electron density map for residues 38–46, calculated using coefficients $(|F_o| - |F_c|)\exp(i\alpha_c)$, where F_o and F_c are the observed and calculated structure factors, and α_c is the calculated phase. Residues 38–46 were omitted in the model used to calculate F_c, which was based on a structure obtained during the terminal stages of the refinement. These residues are an insertion in the TR sequence between residues 53 and 54 in the FAD domain of GR. For clarity, residue 45 is not labeled.

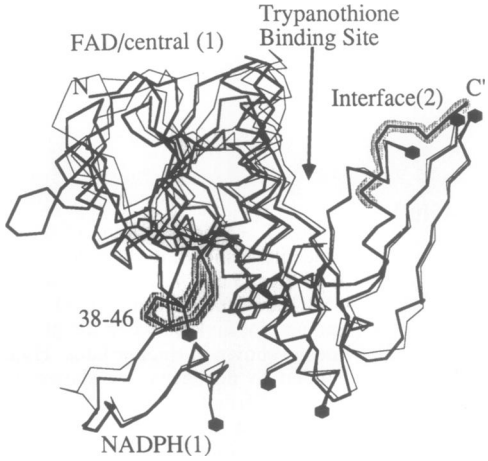

FIG. 3. Active-site region of TR and GR, showing the relative displacements of the FAD and central domains in one monomer. Thick lines, TR; thin lines, GR. The two structures are superimposed using all aligned C_α atoms of the interface domain of the other monomer. C_α atoms are shown for most of the FAD and central domains [marked FAD/central (1)], a small part of the NADPH domain [NADPH (1)] and part of the interface domain of the other monomer in the dimer [Interface (2)]. Chain breaks are indicated by solid hexagons, and the N terminus of the first molecule and the C terminus of the second molecule are marked N and C'. The insertion in the TR sequence (marked 38–46, see Fig. 2) and the C-terminal extension are highlighted by gray shading.

GSSG (14). The x-ray structure of GR complexed with GSSG reveals that the substrate is bound with minimal distortion of the enzyme structure (15). We have chosen, however, to avoid direct comparison of different states of the two enzymes and have placed, for reference, the structure of GSSG (kindly provided by G. E. Schulz, Albert-Lüdwigs Universität, Frieburg, Germany) in the active site of the uncomplexed GR structure. A model for $T(S)_2$ was obtained by simply connecting the two carboxyl groups of the GSSG glycines by an extended spermidine crosslink (Fig. 4), and its orientation and position in the TR active site were determined by reference to the flavin ring system.

Overall Structure. The presence of two molecules in the asymmetric unit provides crystallographically independent views of the two TR monomers and active sites. Except for small deviations at sites of differing intermolecular crystal contact, there are no significant differences between the two. The rms deviation between monomers is 0.4 Å for all C_α atoms. The overall structure of the dimer is very similar to that of GR, relative to which the rms deviation in C_α position is 1.3 Å, including all residues that are aligned in the two sequences (excluding 49 residues in surface loops in each monomer). There are, however, small but significant changes in the interdomain orientations that are seen in both monomers. These are of potential functional importance, as they result in a more open active site in TR relative to GR.

Both monomers of TR superimpose individually onto GR with rms deviations of 1.0 Å, significantly smaller than when aligning the dimers as a unit. This discrepancy arises from a small (2.7°) rotation in the relative orientation of the two molecules in the dimer. A major component of the change in monomer orientation in TR is a 4° rotation of the FAD and central domains away from the interface domain of the other monomer, leading to a $T(S)_2$ binding site that is very similar to that of GR at the base (near the redox-active enzyme disulfide, the FAD group, and the substrate disulfide), but more open by about 4 Å in the region where the spermidine crosslink of $T(S)_2$ is likely to bind (Figs. 3 and 4). The bulk of the opening at the active sites comes from 7° rotations in the orientations of two helices (residues 13–23 and 98–118, Fig. 3). In addition to the FAD and central domains, the NADPH domains are also rotated, by approximately 4°. Subsequent discussion will focus mainly on one of the two active sites, with very similar results being obtained for the other.

Role of Insertions in the TR Sequence. The 9-residue insertion (residues 38–46) in the sequence of TR between GR residues 53 and 54 may play a role in stabilizing the more open active site in TR. This sequence in the FAD domain (His-His-Gly-Pro-Pro-His-Tyr-Ala-Ala, Fig. 3) has a relatively rigid structure because of the two proline residues, and it interacts closely with residues in both the NADPH and FAD domains. Unlike other insertions in the TR sequence, this loop is substantially buried. The solvent-accessible surface area (26) for the loop, calculated using a 1.6-Å probe in the absence of the rest of the protein, is 1197 $Å^2$. In the context of the entire protein structure, the accessible surface area of the loop decreases to 370 $Å^2$; i.e., 69% of the surface area is buried. *T. congolense* TR has a similar insertion (Val-His-Gly-Pro-Pro-Phe-Phe-Ala-Ala) at the same position, as does the *Trypanosoma cruzi* enzyme (27). Of the 16 residues that have atoms within 4 Å of this loop in the *C. fasciculata* structure, 14 are identical in the *T. congolense* sequence, and the other 2 are conservative substitutions.

The other major insertion in the TR sequence (13 residues between residues 133 and 134 in GR) is unlikely to play any role in substrate binding as it is a surface loop located about 30 Å from the active-site disulfide. The first 13 residues of the C-terminal extension in TR are well ordered. Although the C-terminal residue in GR is at the active site, the extension in TR extends away from the active site and is unlikely to interact with the substrate (Fig. 3).

Active Site Structure. There are 48 residues within 8 Å of one of the flavin ring systems of TR; 85% of these residues are identical in TR and GR, including all residues that are involved in the reaction mechanism. The level of sequence identity drops rapidly with distance from the flavin ring system. For residues in the three 1-Å shells between 8 and 11 Å, the identity levels are 64%, 50%, and 41%, respectively. The rms deviation in C_α positions between TR and GR for the residues within 8 Å of the flavin is 0.48 Å—i.e., only slightly higher than the deviation between the two TR monomers (0.4 Å). Structurally conserved residues around the flavin include His-460′ (residue 467′ in GR, the prime referring to a residue in the other subunit), which acts as the active-site base and is held in place by Glu-465′ (472′ in GR), Tyr-197 (197 in GR), which acts as a lid on the flavin in the absence of NADPH, and the ion pair formed by Lys-59 (66 in GR) and Glu-201 (201 in GR), which is presumed to modulate the redox potential of the flavin (14).

Karplus and Schulz (15) have identified the side chains of Ser-30, Arg-37, Tyr-114, Arg-347, His-467′, and Glu-473′ as forming direct hydrogen bonds with GSSG in GR. Of these, only Arg-37 and Arg-347 are missing in TR; in GR they interact with the glycine carboxyls in GSSG that are converted to amide linkages in $T(S)_2$. In addition, five side chains in GR interact with GSSG through water-mediated hydrogen bonds: Lys-67, Tyr-106, Asn-117, Ser-470′, Glu-472′, and Thr-476′ (15). Equivalent residues are present in TR for all except Tyr-106 and Asn-117; the absence of the latter can be rationalized as it interacts with one of the glycine carboxylates of GSSG. Thus, the binding of the γ-Glu-Cys parts of $T(S)_2$ is likely to be very similar to that of GSSG.

Site-directed mutagenesis studies (11–13) have identified three residues as being particularly important for discriminating between $T(S)_2$ and GSSG: Glu-17 (Ala-34 in GR), Trp-20 (Arg-37), and Ala-342 (Arg-347). In the x-ray structure of TR, the side chains of Trp-20 and Met-112 (Asn-116 in GR) provide a hydrophobic pocket that is positioned to bind the spermidine in the model, with no unfavorably close contacts

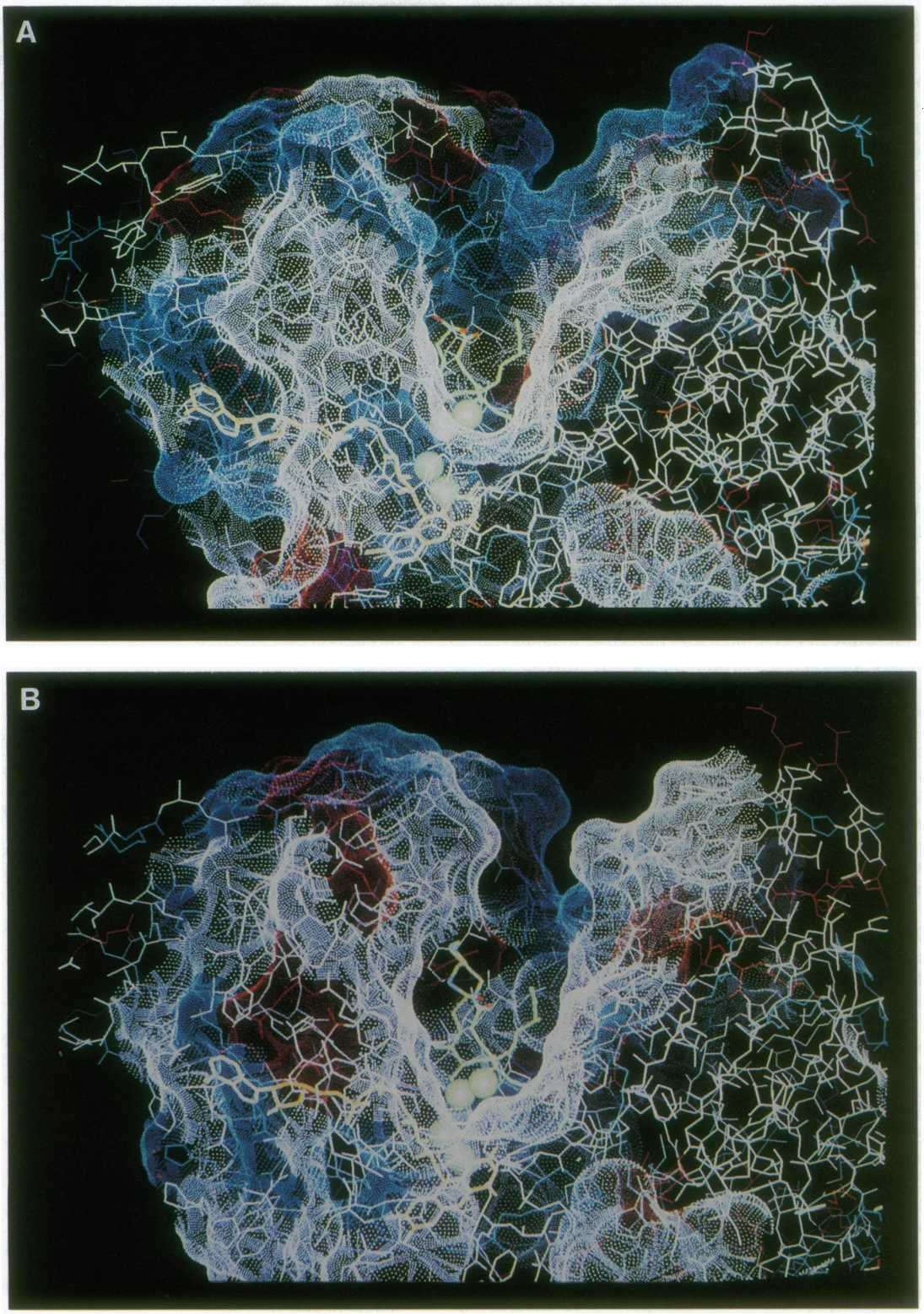

FIG. 4. Solvent-accessible surfaces (26) of the active-site regions of GR (*A*) and TR (*B*). Color reflects the nature of the nearest amino acid residue, with blue denoting arginine, lysine, or histidine and red denoting aspartic acid or glutamic acid. All other residues are colored white. The FAD groups are shown with thicker bonds and colored yellow. The green spheres denote the redox-active sulfurs of the enzyme (below) and the substrate (above). The structure of GR is that of Karplus and Schulz (14) for the uncomplexed enzyme. The models for GSSG and $T(S)_2$ (thick green bonds) are based on the structure of the GR enzyme–substrate complex (15) and are for reference only. Note that the active site is significantly wider in TR around the $T(S)_2$ model. There are two protrusions at the outer edges of the TR binding site that lead to a more closed-off appearance relative to GR. One protrusion is due to a single residue insertion in TR between GR residues 42 and 43 that causes several residues, including TR Leu-25, to bulge out. The other protrusion is due to the C-terminal extension.

and with a nice stacking of the spermidine along the long axis of the tryptophan ring system (Fig. 4*B*). Likewise, the carboxyl group of Glu-17 in the TR x-ray structure is positioned to hydrogen bond with the amide nitrogen of the

spermidine linkage. It is unlikely to interact directly with the positively charged amino group of the linker, being ≈7 Å or 5.5 Å from it in the model, depending on the orientation of the linker. Ala-342 in TR replaces Arg-347, which interacts the glycine carboxyls of GSSG in GR.

Fig. 4 shows the solvent-accessible surfaces at the substrate binding sites of GR and TR. The most striking difference between the two arises from differences in the distribution of charged residues. An array of positively charged residues in GR (Fig. 4*A*) is absent in TR, which has instead a mixture of mainly neutral and some negatively charged residues in the corresponding region (Fig. 4*B*). The closest charged residues to the model-built spermidine linkage are Glu-17 (Ala-34 in GR) and Asp-115 (Lys-120 in GR). No other negatively charged groups are present within interaction distance of the amide linkage to the spermidine or the spermidine linkage itself. The closest basic groups are the side chains of Arg-354, Arg-471′, and His-26, which are all more than 12 Å away and are unlikely to interact directly. This is in contrast to the binding site in GR, where a cluster of positively charged residues is adjacent to the negatively charged glycine carboxyls of the two GSSG tripeptides. These include Arg-37, Arg-38, Lys-120, Arg-347, Lys-348, His-351, and Arg-478′. Arg-478′ (corresponding to Arg-471′ in TR) forms an ion pair with Glu-41 that keeps it positioned near the GSSG binding site. The glutamic acid is lacking in TR, and Arg-471′ points away from the active site.

The overall impression obtained on comparing the two substrate binding sites of the human and parasite enzymes is that the strongly charged environment of the former is replaced by an essentially neutral binding site in TR. An important feature of the TR binding site is a pocket formed by the terminal methyl group of Met-112 and the side chains of Leu-16, Tyr-109, Trp-20, and Glu-17. The pocket is mainly hydrophobic but with a negatively charged patch formed by the carboxyl groups of Glu-17. Interestingly, analogs of $T(S)_2$ with increased aliphatic character (i.e., where the spermidine moiety is replaced by an aliphatic side chain with only one amine function) are good substrates for the enzyme (7).

These results are consistent with conclusions drawn from site-directed mutagenesis studies and molecular modeling of TR and GR (10–13). Walsh and coworkers (11) have replaced three residues in *T. congolense* TR (Asp-18, Trp-21, and Ala-343) by the corresponding residues in human GR (Ala-34, Arg-37, and Arg-347) and have obtained an enzyme midway between TR and GR in terms of its turnover number for GSSG (12). Replacement of the same residues in human GR by their TR equivalents results in the acquisition of TR activity and a substantial decrease in GSSG turnover (13). Perham and coworkers (11) have likewise switched the substrate specificity of *Escherichia coli* GR from GSSG to $T(S)_2$ by introducing similar changes.

The active-site region is not blocked by intermolecular contacts in the crystal form studied, making possible the determination of structures of the enzyme complexed with substrates and inhibitors (J. L. Martin, X.-P.K., T.S.R.K., A.C., J.K., unpublished data). A crystal (form III) was soaked in 3 mM $T(S)_2$ (Bachem, trifluoroacetic acid salt) for 12 hr. X-ray data to 2.6-Å resolution were measured using a Rigaku R-AXIS IIC image-plate area detector. A difference Fourier map ($|F_o| - |F_c|$), using phases calculated from the model for the uncomplexed enzyme and F_o from this experiment, revealed strong electron density at the active site, the only region of significant electron density in the map. Preliminary refinement indicates that the enzyme in this crystal form does not undergo a significant conformational change upon substrate binding and confirms that the substrate binds in a conformation similar to that of GSSG in GR (J. L. Martin *et al.*, unpublished data). Additional structural information is also expected to be available for a *P*4(3)22 crystal form of *C. fasciculata* TR (28) and for crystals of the enzyme from *T. cruzi* (27, 29). Comparison of these structures should clarify the role of the domain rotations in stabilizing the enzyme–$T(S)_2$ complex and will provide a consensus template for the subsequent design of specific inhibitors of the parasite enzyme.

This paper is dedicated to the memory of G.B.H. We thank Stephen K. Burley and Elias Lolis for their extremely valuable assistance with the data collection as well as for helpful discussions. We are grateful to Richard Perham and Christopher T. Walsh for providing data in advance of publication. This work was supported in part by grants from the National Institutes of Health (GM45547 to J.K., AI19428 to A.C., and AI26784 to G.B.H.). J.K. is a Pew Scholar in the Biomedical Sciences. Beamline X12-C of the National Synchrotron Light Source at Brookhaven National Laboratory is funded by the Office of Health and Environmental Research of the U.S. Department of Energy.

1. Fairlamb, A. H. (1981) *Trends Biochem. Sci.* **7**, 249–253.
2. Fairlamb, A. H., Blackburn, P., Ulrich, P., Chait, B. T. & Cerami, A. (1985) *Science* **227**, 1485–1487.
3. Schirmer, R. H. & Schulz, G. E. (1987) *Pyridine Nucleotide Coenzymes Part B (Coenzymes and Cofactors)*, eds. Dolphin, D., Poulson, R. & Avramovic, O. (Wiley, New York), Vol. 2.
4. Karplus, P. A., Pai, E. F. & Schulz, G. E. (1989) *Eur. J. Biochem.* **178**, 693–703.
5. Shames, S. L., Fairlamb, A. H., Cerami, A. & Walsh, C. T. (1986) *Biochemistry* **25**, 3519–3526.
6. Field, H., Cerami, A. & Henderson, G. B. (1991) *Mol. Biochem. Parasitol.*, in press.
7. Henderson, G. B., Fairlamb, A. H., Ulrich, P. & Cerami, A. (1987) *Biochemistry* **27**, 3023–3027.
8. Meshnick, S. R., Blobstein, S. H., Grady, R. W. & Cerami, A. (1978) *J. Exp. Med.* **148**, 569–579.
9. Arrick, B. A., Griffith, O. W. & Cerami, A. (1981) *J. Exp. Med.* **153**, 720–725.
10. Murgolo, N. J., Cerami, A. & Henderson, G. B. (1990) *Ann. N.Y. Acad. Sci.* **569**, 193–200.
11. Henderson, G. B., Murgolo, N. J., Kuriyan, J., Ösapay, K., Kominos, D., Berry, A., Scrutton, N. S., Hinchcliffe, N. W., Perham, R. N. & Cerami, A. (1991) *Proc. Natl. Acad. Sci. USA* **88**, 8769–8773.
12. Sullivan, F. X., Sobolov, S. B., Bradley, M. & Walsh, C. T. (1991) *Biochemistry* **30**, 2761–2767.
13. Bradley, M., Bücheler, U. S. & Walsh, C. T. (1991) *Biochemistry*, in press.
14. Karplus, P. A. & Schulz, G. E. (1987) *J. Mol. Biol.* **195**, 701–729.
15. Karplus, P. A. & Schulz, G. E. (1989) *J. Mol. Biol.* **210**, 163–180.
16. Kuriyan, J., Wong, L., Guenther, B. D., Murgolo, N. J., Cerami, A. & Henderson, G. B. (1990) *J. Mol. Biol.* **215**, 335–337.
17. Messerschmidt, A. & Pflugrath, J. W. (1987) *J. Appl. Cryst.* **20**, 306–315.
18. Kabsch, W. (1988) *J. Appl. Cryst.* **21**, 916–924.
19. Brünger, A. T. (1990) *Acta Crystallogr. Sect. A.* **46**, 46–57.
20. Fitzgerald, P. M. D. (1988) *J. Appl. Crystallogr.* **21**, 273–278.
21. Jones, T. A. & Thirup, S. (1986) *EMBO J.* **5**, 819–822.
22. Brünger, A. T. (1988) X-PLOR (The Howard Hughes Medical Institute and Dept. Molecular Biophysics and Biochemistry, Yale Univ., New Haven, CT), Version 1.5, Manual.
23. Brünger, A. T., Kuriyan, J. & Karplus, M. (1987) *Science* **235**, 458–460.
24. Weis, W. I., Brünger, A. T., Skehel, J. J. & Wiley, D. C. (1990) *J. Mol. Biol.* **212**, 737–761.
25. Shames, S. L., Kimmel, B. E., Peoples, O. P., Agabian, N. & Walsh, C. T. (1988) *Biochemistry* **27**, 5014–5019.
26. Lee, B. K. & Richards, F. M. (1971) *J. Mol. Biol.* **55**, 379–400.
27. Sullivan, F. X. & Walsh, C. T. (1991) *Mol. Biochem. Parasitol.* **44**, 145–148.
28. Hunter, W. N., Smith, K., Derewenda, Z., Harrop, S. J., Habash, J., Islam, M. S., Helliwell, J. R. & Fairlamb, A. H. (1990) *J. Mol. Biol.* **216**, 235–237.
29. Krauth-Siegel, R. L., Enders, B., Henderson, G. B., Fairlamb, A. H. & Schirmer, R. H. (1987) *Eur. J. Biochem.* **164**, 123–128.